Atomic Force Microscopy of Biomaterials, Mica, and the Origins of Life

Helen Greenwood Hansma[1] * and Emin Oroudjev[2]

[1]Department of Physics, University of California, Santa Barbara, CA 93106
[2]Department of Molecular, Cellular, and Developmental Biology, University of California, Santa Barbara, CA 93106

* helen.hansma@gmail.com

Introduction

Atomic force microscopy (AFM) began as an art as well as a science, and in many ways it continues to be an art and a science. Despite the existence of new, better, faster, bigger (or smaller!) atomic force microscopes (AFMs), some of the of the fundamental challenges remain—probe tips, sample dirt, and moving beyond leading-edge results obtained with one biological system to obtain leading-edge results with a related system.

With regard to sample preparation, some methodological approaches are easily communicated. Other approaches are often nearly subconscious, such as the choice of rinsing a sample with a stream of water directed directly at the sample spot or directed above the sample spot, such that the water flows more gently over the sample spot. This can result in very different surface coverages, such that one person's samples will have many DNA molecules per square micron, whereas another person's samples will have only an occasional DNA molecule.

Different regions of the same sample can appear very different. In one early experiment, our samples of DNA with a single-stranded binding protein showed only a solid "lawn" of material. By imaging progressively farther from the center of the sample, we eventually came upon a region where the lawn ended and individual molecules of DNA coated with single-stranded binding protein were seen.

Operation of AFMs is also a combination of art and science that involves learning general rules for cantilever tuning, imaging forces, speeds, and gains and then manipulating these variables to optimize the imaging of the specific sample under the cantilever's probe tip.

Exciting breakthroughs were made in some of our earliest work, such as the time-lapse movie of fibrin polymerization [1] and reproducible imaging of DNA under propanol (Figure 1A) [2]. Later research included time-lapse movies of DNA (Figures 1B & 2) [3, 4], other research on DNA (Figure 1C) [5–8], the extracellular matrix [9, 10], synaptic vesicles [11, 12], analyses of bacterial biofilms [13, 14], and pulling on spider silk [15, 16]. AFM methods for imaging in fluid are presented in Kindt et al.'s article in *Methods in Cell Biology* [17], which is part of a useful volume about AFM methods in cell biology [18]. Several reviews by members of our lab have appeared therein [19–21].

Results

Fly eye. An undergraduate in the lab caught a fly, and Oroudjev removed the eye, mounted it, and imaged it by AFM. Individual ommatidia in the compound eye of the fly are ~20 μm wide and ~3 μm high (Figure 3). The surfaces of the ommatidia are covered with aperiodic arrays of substructures, as seen in amplitude and phase images from tapping-mode AFM (Figure 4). These substructures have been described as a cerebral cortex-like pattern of ridges in earlier AFM images [22].

Collagenous extracellular matrix (ECM) from osteoblasts. Osteoblasts are bone-building cells that produce large quantities of extracellular collagen. Extracellular matrix from cultured osteoblasts was treated to remove calcium, as outlined in the caption of Figure 5. Collagen fibrils in the ECM can be identified by their strong banding, with 64- to 65-nm periodicities and weaker banding with 32–33 nm. The 2×2 μm amplitude image inset in Figure 5B shows a region almost completely covered with nearly parallel collagen fibrils.

Probe tips—still a holy grail of AFM research. Imagine that the AFM could reliably image sequence-dependent substructure on DNA at the level of the double-helix. This appears to have been done in a small series of images from our lab in the mid-1990s. Figure 6 is one of these images. This image was taken with an early prototype AFM for tapping in fluid
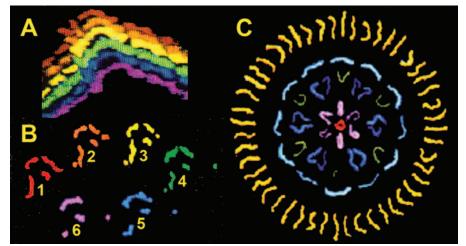

Figure 1: Colorful early AFM of DNA. (A) In this 1991 *Science* cover article [2], simply imaging DNA reproducibly was an accomplishment. Six successive images of DNA are colorized and arranged with the first image on top and the last image on the bottom. Pixelation is an artifact of the computer monitor. (B) DNase degradation of DNA is the easiest enzymatic reaction to observe in the AFM, using a non-specific DNA endonuclease such as DNase [3]. Images 1-6 show successive degradation of DNA over ~15 minutes (C) "DNA on Drugs." Mandala of 400 base-pair (bp) DNA images from an AFM shows an outer circle of yellow DNA without drug, surrounding variously bent and colored DNA molecules in the inner circles. DNA molecules in the inner circles were imaged in the presence of a "drug" composed of a polyamine that binds to DNA's phosphate backbone and a tri-pyrrole peptide that binds to DNA's minor groove [5].
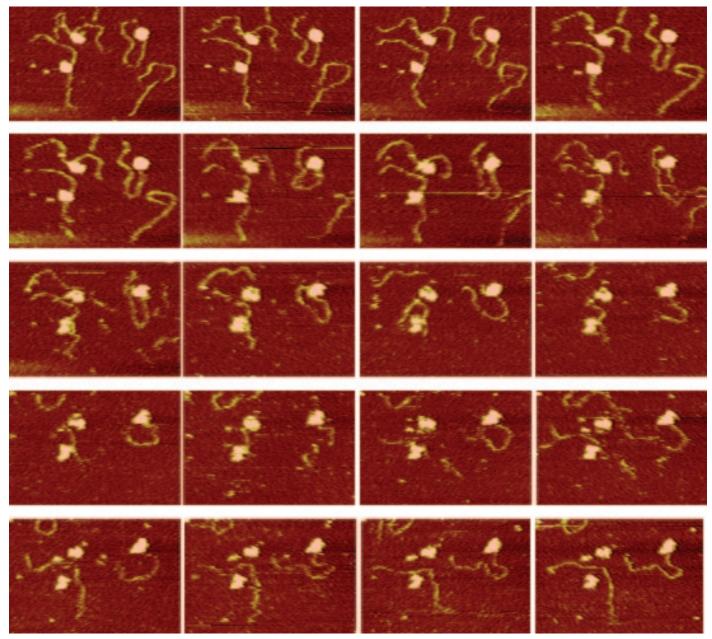
Figure 2: DNA "swimming" in the AFM. The DNA is in complexes with *E. coli* RNA polymerase (RNAP). Successive images are in horizontal rows, from top to bottom. The 3 RNAP "blobs" stay in the same place throughout these images, captured at 42-second intervals, while the 4 DNA molecules move around a lot and disappear from the field of view, in the case of the top left and bottom right DNA molecule in the first image. At the end, both of the 2 RNAP molecules originally attached near the centers of DNA molecules have lost their DNA. DNA length is 1047 bp. Images are 330 × 495 nm. See [24] for further detail.

that never became commercial. The silicon-nitride V-shaped cantilever used for the image had a "super tip" grown at the tip of the cantilever's tip by electron beam deposition (EBD) in a scanning electron microscope (SEM). The super tip started out as an unimpressive tip, giving apparent DNA widths of ~7 nm. After several images, the apparent width of the DNA changed to that seen in Figure 6, with an apparent width of only 2–3 nm, like the diameter of the DNA double helix by x-ray crystallography. After a half dozen scans, the apparent width of the dsDNA again became too broad to resolve helix turns [21].

Each AFM tip is unique and changes even during use, as it picks up or loses material. Some of the best and sharpest AFM tips were the early glued diamond tips, in which a shard of diamond was glued to a tipless cantilever, using an eyebrow hair to maneuver the glue and the diamond onto the cantilever [1]. When carbon nanotubes were discovered, there was great hope that these would soon be standing on top of the tips on cantilevers. Twenty years later, there is still much room for improvement.

One approach that was sometimes useful for improving tips was to move to an "unimportant" area of the sample and image at high speed and high force. Although this might be expected to dull the tip, in many cases it actually improved the image quality, as determined by the width (narrowness) of small features.

Mica. The samples above, except for the fly eye, were all imaged on mica, which is a layered aluminosilicate mineral
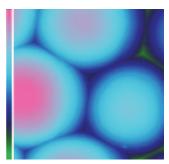
Figure 3: Fly Eye. 30-μm height image of ommatidia in the compound eye from a fly that appeared to be a housefly, *Musca domestica*. AFM in air. Z-scale bar on the left = 6 μm from green (low) to pink (high).

with perfect cleavage planes. The sheets of mica are held together by potassium ions, which are also present in ~100-mM concentrations in the cytoplasms of all cells. One of mica's advantages is that it is atomically flat, thus allowing one to see even bare DNA molecules as ridges above the mica surface.

Possible origin of life between mica sheets. An unexpected offshoot of biological AFM has been the hypothesis that life might have originated between mica sheets (Figure 7) [23]. The spaces between mica sheets provide many adjacent chambers or "cells" in which pre-cellular life could have developed, in an environment rich in potassium ions and low in entropy. Mica also provides an endless energy source—mechanical energy or work—that might have been used to form covalent bonds, restructure polymers, and bleb daughter cells off the earliest protocells.

Mica's affinity for biomolecules provides supporting evidence that life could originate in a "Mica World," as proposed in the mica hypothesis above. Mica's affinity for biomolecules can be seen especially in Figures 2 and 8. DNA (Figure 2) and two very different proteins—laminin (Figure 8) and RNA polymerase (Figure 2)—bind to mica. Both DNA and laminin move on the mica surface (Figures 2 and 8). The binding of DNA to mica is strengthened or weakened in the presence of different divalent inorganic cations commonly found in living systems [12].
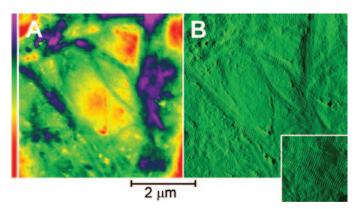

Figure 5: Collagen-rich extracellular matrix from cultured osteoblasts. (A) Height image. (B) Amplitude images. Osteoblasts were cultured on mica for 1 month and then washed with water to lyse the cells. The resulting ECM was peeled off the mica and inverted onto another piece of mica so that the smooth side was facing up. The ECM was treated for 20 seconds with an EDTA solution and rinsed 3 times with water to remove calcium revealing an ECM rich in collagen fibrils. Z-scale on left = 150 nm from red (low) to purple (high) for height image.

New techniques in microscopy and microanalysis might be necessary for acquiring direct new evidence for the mica hypothesis. It might be possible to synthesize biomolecules between mica sheets by mechanochemistry, using the work from moving mica sheets. However, any newly synthesized molecules would be present in only sub-monolayer quantities, and the molecules would be *between* the mica sheets as opposed to on top of them. Detecting and analyzing these molecules would be done best with techniques that could ablate successive layers of mica and then analyze the molecules on the surfaces of the newly exposed mica sheets. *Micro*-analysis would be orders of magnitude too insensitive to detect these sub-monolayers of molecules. What would be needed is something more
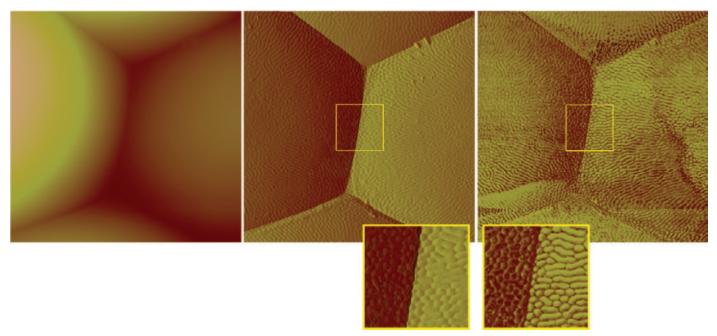

Figure 4: Fly Eye. 15-μm images are height (left), amplitude (middle), phase (right). Z-scale on left = 8 μm from brown (low) to white (high) for height image. Yellow-bordered insets are enlargements of the regions of the amplitude and phase images shown by the yellow squares on these images. Aperiodic substructures in amplitude and phase images have nearly constant widths of ~230–240 nm and lengths ranging from ~230 nm to nearly 3 μm.
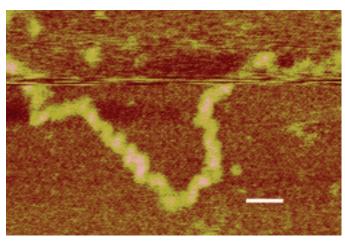
Figure 6: Helix turns in double-stranded DNA. This AFM image of DNA in propanol shows a right-handed double-helix [21, 25]. Scale bar = 5 nm.
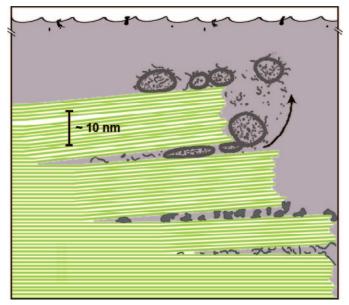

Figure 7: Could life have evolved between mica sheets? Diagram of a "Mica World" in a dark primitive ocean from a time when the sky was not yet blue. The mica sheets are green lines, and the gray structures are various ancient biological molecules and lipid vesicles. Potassium in the white lines holds the green mica sheets together. In the mica hypothesis, water moves in and out of the spaces between stacks of sheets, and the sheets move up and down and do work on the gray structures between the sheets. Work is a type of energy that might be able to push molecules together to form covalent bonds. The curved arrow shows how the mica sheets might squeeze lipid vesicles and pinch off pieces of them in a pre-biotic form of cell division [23]. Scale bar (10 nm) is the height of 10 mica sheets.

like *zepto*-analysis. In the meantime, our evidence that life could originate in a "Mica World" is more limited, relying on evidence such as mica's affinity for biomolecules and other supporting evidence described in [23].
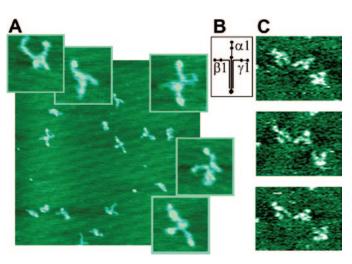
Acknowledgments

Figure 8: Laminin protein molecules on mica: (A) in air, and (C) in motion under aqueous fluid. A. A 1×1 micron field of laminin molecules with enlarged images of 5 laminin molecules. B. Structural diagram of a laminin molecule, which is a cross-shaped molecule composed of 3 protein chains, $\alpha 1$, $\beta 1$, and $\gamma 1$. C. Three sequential images of 3 laminin molecules waving their arms on mica. Each image is 280×210 nm. For further detail, see [9].

References

[1] B Drake et al., *Science* 243(4898) (1989) 1586–89.
[2] HG Hansma et al., *Science* 256 (1992) 1180–1184.
[3] M Bezanilla et al., *Biophys J* 67 (1994) 2454–59.
[4] M Argaman et al., *Nucleic Acids Res* 25 (1997) 4379–84.
[5] HG Hansma et al., *Biochemistry* 33 (1994) 8436–41.
[6] HG Hansma and DE Laney, *Biophys J* 70 (1996) 1933–39.
[7] R Golan et al., *Biochemistry* 38 (1999) 14069–76.
[8] JC Sitko, EM Mateescu, and HG Hansma, *Biophys J* 84 (2003) 419–31.
[9] CH Chen, DO Clegg, and HG Hansma, *Biochem* 37 (1998) 8262–67.
[10] CH Chen and HG Hansma, *J Struct Biol* 131 (2000) 44–55.
[11] RA Garcia et al., *J Neuroscience Res* 52 (1998) 350–55.
[12] DE Laney et al., *Biophys J* 72 (1997) 806–13.
[13] I Auerbach et al., *J Bacteriol* 182(13) (2000) 3809–15.
[14] RE Steinberger et al., *Microbial Ecology* 43(4) (2002) 416–23.
[15] N Becker et al., *Nature Materials* 2 (2003) 278–83.
[16] E Oroudjev et al., *Proc Natl Acad Sci USA* 99 (2002) 6460–65.
[17] JH Kindt et al., *Methods Cell Biol* 68 (2002) 213–29.
[18] BP Jena and JKH Horber, *Methods in Cell Biology* vol. 68, eds. L Wilson and P Matsudaira, Amsterdam, Academic Press, 2002.
[19] HG Hansma and J Hoh, *Annu Rev Bioph Biom* 23 (1994) 115–39.
[20] HG Hansma et al., *J Struct Biol* 119(2) (1997) 99–108.
[21] HG Hansma, *Annu Rev Phys Chem* 52 (2001) 71–92.
[22] MS Anderson and SD Gaimari, *J Struct Biol* 142(3) (2003) 364–68.
[23] HG Hansma, *J Theor Biol* 266(1) (2010) 175–88.
[24] HG Hansma, *Proc Natl Acad Sci USA* 96 (1999) 14678–80.
[25] HG Hansma et al., *Biophys J* 68 (1995) 1672–77.

MT

Scanning Electron Microscopes

VEGA 3

Introducing New Generation of SEMs

After 10 years of continuous development, VEGA matured into its 3rd generation. The VEGA 3 series were designed with respect to a wide range of SEM applications and needs in today's research and industry and provides users an advantage of the latest technology.

Key features of the VEGA 3 Generation:

- A new high-performance electronics for faster image acquisition and signal processing
- Ultra-fast scanning system with compensation of static and dynamic image aberrations
- An extended range of scanning modes using the original Wide Field Optics™
- Unique Tescan In-Flight Beam Tracing™ for real-time beam current and spot size optimization
- Full software control and high level of automation without any mechanical adjustments
- Built-in scripting for user defined applications

TESCAN

PERFORMANCE IN NANOSPACE

Tescan USA
508 Thomson Park Drive
Cranberry Twp., PA 16066
Phone: 724-772-7433
Email: info@tescan-usa.com

www.tescan.com